Assessment of a Novel Position Verification Sensor to Identify and Isolate Robot Workcell Health Degradation

Brian A. Weiss
Intelligent Systems Division,
National Institute of Standards and Technology (NIST),
Gaithersburg, MD 20899
e-mail: brian.weiss@nist.gov

Jared Kaplan
Intelligent Systems Division,
National Institute of Standards and Technology (NIST),
Gaithersburg, MD 20899
e-mail: jared.kaplan@nist.gov

Manufacturing processes have become increasingly sophisticated leading to greater usage of robotics. Sustaining successful manufacturing robotic operations requires a strategic maintenance program. Without careful planning, maintenance can be very costly. To reduce maintenance costs, manufacturers are exploring how they can assess the health of their robot workcell operations to enhance their maintenance strategies. Effective health assessment relies upon capturing appropriate data and generating intelligence from the workcell. Multiple data streams relevant to a robot workcell may be available including robot controller data, a supervisory programmable logic controller data, maintenance logs, process and part quality data, and equipment and process fault and failure data. These data streams can be extremely informative, yet the massive volume and complexity of this data can be overwhelming, confusing, and sometimes paralyzing. Researchers at the National Institute of Standards and Technology have developed a test method and companion sensor to assess the health of robot workcells which will yield an additional and unique data stream. The intent is that this data stream can either serve as a surrogate for larger data volumes to reduce the data collection and analysis burden on the manufacturer, or add more intelligence to assessing robot workcell health. This article presents the most recent effort focused on verifying the companion sensor. Results of the verification test process are discussed along with preliminary results of the sensor's performance during verification testing. Lessons learned indicate that the test process can be an effective means of quantifying the sensor's measurement capability particularly after test process anomalies are addressed in future efforts. [DOI: 10.1115/1.4048446]

Keywords: degradation, monitoring and diagnostics, industrial robot systems, kinematics, manufacturing, monitoring, prognostics, prognostics and health management (PHM), use cases, verification, workcell, metrology, robotics and flexible tooling, sensors

1 Introduction

Every product used in daily life is manufactured in some way, from the clothes that are worn, to the automobiles that are driven, and the cell phones that are used. Each of these products, and many more, are being offered with more customizable configurations and options. Coupling the concept of product customization with the evolution of manufacturing technologies has led to manufacturing processes becoming increasingly flexible and complex [1–3]. To enable greater flexibility and handle increased task complexity, manufacturers have turned to robotic technologies. Robots can offer manufacturers numerous benefits (e.g., increase accuracy, precision, repeatability, and efficiency) as compared to conventional manufacturing automation or manual capabilities [4–6].

As robots have become more adept at providing a broader range of manufacturing capabilities, they are presenting more operational complexity. More complexity typically leads to greater opportunity for faults and failures in the process and equipment. In turn, this spurs more unplanned maintenance or more planned maintenance routines to lessen the potential for unexpected faults or failures [7–9]. Manufacturers, from small to large, recognize that strategic and scripted maintenance strategies are critical to maximize process and equipment availability [10,11].

Personnel from the National Institute of Standards and Technology (NIST) are conducting research to develop measurement science products (e.g., test methods, performance metrics, and reference data sets) to promote the verification and validation of monitoring, diagnostic, and prognostic technologies within manufacturing operations as part of NIST's Smart Manufacturing programs [12–14]. These measurement science products are intended to decrease equipment and process downtime and increase reliability for smart manufacturing systems. A critical output of the effort is the dissemination and adoption of these products by the manufacturing community. A specific measurement science product being developed is a test method, along with a companion sensor to be used within the test method, to assess the degradation of the workcell's kinematic chain (i.e., the assembly of individual rigid bodies at joints) [15,16]. When applied by industry to operational manufacturing robot workcells, the test method can identify and isolate degradations, within the workcell, which are negatively impacting the accuracy of the process. Ultimately, the test method, along with the sensor, will be made publicly available to industry for widespread adoption and implementation. Before this can be achieved, the overall test method, including the sensor, requires testing and verification.

This publication presents NIST's latest efforts to verify the performance of the companion sensor. Early work focused on manually testing the sensor. This proved overly time-consuming and prone to human error. Current efforts have focused on automating the testing process to cover more test points in a faster manner, as compared to manual testing. The remainder of this article is organized as follows. Section 2 presents the motivation for this effort.

Manuscript received May 26, 2020; final manuscript received May 29, 2020; published online November 10, 2020. Assoc. Editor: Y. Lawrence Yao.

Section 3 describes the test method in detail and discusses how the sensor is integrated with the test method. Section 4 describes the design and development of the automated measurement test stand. Section 5 highlights the tests that were conducted and Sec. 6 analyzes the preliminary results from two perspectives—how well did the automated measurement testing process perform and how well did the companion sensor perform. Lastly, Sec. 7 describes the expected next steps of this research effort.

2 Background

Maintenance is typically a critical factor to ensure long-term, acceptable operation for any process or piece of equipment. Although important, maintenance can be expensive and cumbersome [17,18]. Without sufficient intelligence regarding the health of their manufacturing operation, which would include resident robot workcells (defined to include the robot, end-of-arm tooling, sensors, controller(s), and other supporting automation), manufacturers cannot make informed decisions about the most cost-effective and efficient maintenance strategy(ies) by which to maintain their operations. The discipline of monitoring, diagnostics, and prognostics to enhance decision-making surrounding maintenance activities is known as prognostics and health management (PHM) [19–22]. The optimal maintenance schedule includes striking a balance between preventative maintenance (PM) (performing specific maintenance activities at set intervals of time, cycles, or other measurable unit) and predictive maintenance (PdM) (performing specific maintenance activities only when the current condition of equipment predicts that maintenance is necessary) all in an effort to minimize reactive maintenance (RM) ("fix it when it breaks") [23]. Preventive maintenance can become excessive leading to wasted time and money. However, minimizing or trivializing preventive maintenance can lead to too much of reactive maintenance. Unexpected shutdowns resulting from reactive maintenance can lead to loss of revenue and loss of customers.

Tracking the health of robot workcells allows manufacturers to make informed decisions about the type of maintenance needed and the schedule at which it should be performed. Data are required to generate intelligence regarding robot workcell health. Multiple data streams are likely to exist that are relevant to identifying the health of a robot workcell. They include the following:

- Robot-level data—Many robot controllers capture a range of information including robot joint and tool-center positions, velocities, and accelerations; joint temperatures; joint currents; and joint voltages. These data are usually quantitative.
- Process-level data—This type of data could be captured from the overall process controller or from a supervisory Programmable Logic Controller (PLC). Time data are an example of process-level data, where time can include overall task time, sub-task time, and takt time. These data are usually quantitative.
- Quality data—These data are measured from the part produced once the workcell has completed its operation. These data could be quantitative or qualitative.
- Operational configuration data—This data type includes information describing the workcell's configuration and operations. This can include the make and model of equipment, technologies, and sensors critical to the workcell's function. This information can also describe the workcell's operation (e.g., Robot Arm 01 lifts a 2 kg box, puts it down, then lifts a 5 kg box, and puts it down). This can be both quantitative and qualitative descriptive data.
- Fault and failure data—For any fault or failure that presents itself within a manufacturing operation, it is almost always documented. This documentation could be done by multiple individuals including the equipment and process operator, maintenance technician, or supervisor. Fault and failure data can be quantitative from sensor and equipment readings (e.g., the current peaked at 18 A). It can also be descriptive—e.g., smoke started rising from the motor, I then heard a loud crack, and the motor stopped running.
- Maintenance logs—Most manufacturers document their maintenance activities, whether it results from planned maintenance (predictive or preventive) or from unplanned maintenance (reactive). Maintenance records can include what specific work was performed and a description of the restorative state that the equipment is now in.

Effectively turning all of these data into health intelligence is nontrivial, especially as it relates to robot workcells [24]. Multiple algorithms exist that dictate how to fuse or analyze the data to discover new intelligence. Each method comes with its advantages and disadvantages. Generating the appropriate amount of intelligence can be paramount to an organization. Too little intelligence can lead to vast uncertainty and present an excessive amount of options to maintenance decision-makers. An over-abundance of intelligence can be costly, both in the time to generate and required resources. For highly critical processes or equipment, a cost–benefit analysis could dictate the need for more, as opposed to less, intelligence. The right amount of intelligence can prevent degradations that force part quality or process productivity to unacceptable levels while still promoting cost-effective operations [25,26]. NIST has developed the *Identification and Isolation of Robot Workcell Accuracy Degradation* test method and companion Position Verification Sensor with Discrete Output (U.S. Patent Pending, Serial Number 16/572,847) to provide a new stream of direct intelligence that can localize where faults and failures are occurring in a workcell's kinematic chain, and offer additional data that can be fused with the afore-mentioned data to offer a richer understanding of the workcell's health. The following section describes the test method, position verification sensor, and the need for sensor verification.

3 Test Method and Sensor Description

The *Identification and Isolation of Robot Workcell Accuracy Degradation* test method was developed in concert with a multi-robot testbed at NIST [27]. Figure 1 presents the NIST's PHM for Robot Systems testbed with many representative features of a manufacturing robot workcell including robots, controllers, and end-of-arm tools. The testbed features two six degrees-of-freedom (6DOF) Universal Robots, each with industrial controllers. The smaller robot, a UR3 (shown on the left in Fig. 1), is configured to perform path-planning operations including drawing several unique patterns while the larger robot, a UR5 (shown on the right in Fig. 1), is configured to perform a material handling operation. The UR3 is configured with a pen at its tool-center-position using a specially designed mount. The UR5 is configured with an RG2 gripper that is controlled through the UR5's controller. Supervisory commands are issued to both the UR3 and the UR5 by a single Beckhoff PLC.

The testbed's primary manufacturing-relevant use case is for the larger robot to physically place test parts on fixtures within the reach of the path-planning robot for this smaller robot to draw on the test part. This drawing activity is analogous to welding, adhesive application, and additive manufacturing processes performed by six-degree-of-freedom robot systems. Additional information on the testbed and use case is shown in Refs. [15,27]

The *Identification and Isolation of Robot Workcell Accuracy Degradation* test method involves testing the positioning repeatability, and therefore the health, of different components along the robot workcell's kinematic chain. The test method uses the NIST-developed Position Verification Sensor with Discrete Output (PVS) sensor (depicted in Fig. 2) to measure the positioning of the components in question [16]. The test method is robot agnostic; it can be integrated and executed with any 6DOF robot workcell. When different measurement points along the kinematic chain are tested, the test method's results aim to isolate any source(s) of the error, so the responsible component can be appropriately addressed. Implementing the test method first involves

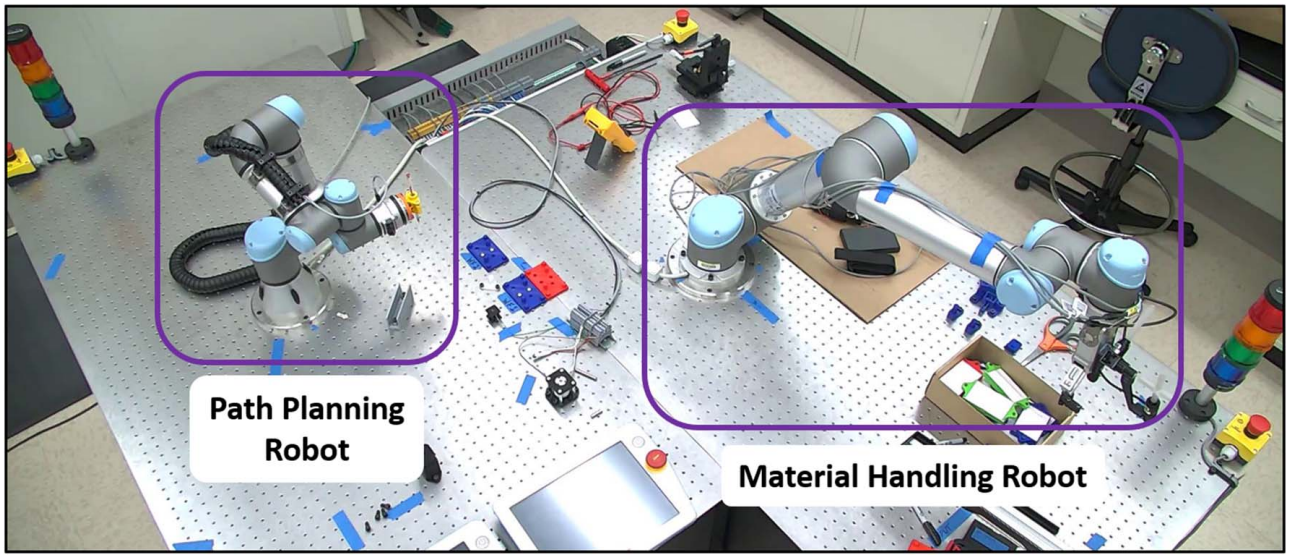

Fig. 1 NIST PHM for robot systems testbed

affixing mechanical keys at strategic locations along the workcell's kinematic chain that can present positional degradation. The PVS is physically installed within the workcell's work volume. The keys are commercial-off-the-shelf (COTS) items with precise geometries. The dimensions of the keys are in English units so the sensor's clearance dimension is manufactured in English units.

In the case of the NIST testbed, keys have been attached to multiple elements including the robot's tool flange, physical mount of the gripper jaws, and the movable gripper jaws, themselves (shown in Fig. 3). Once the keys are installed, the robot, along with the other movable elements in the kinematic chain (e.g., gripper), is systematically programmed to "insert" their keys into the PVS. The PVS is designed such that the key can be successfully inserted within a specific tolerance as determined by the dimensions of the key and the opening of the PVS. If the key's position is inaccurate beyond the tolerance of the PVS' opening, then the test of that specific point will fail. Otherwise, if the movement of the key is within the tolerance of the PVS' opening, then the key will be successfully inserted into the PVS and this specific point will pass. The element to which the key is attached when a failure is observed highlights the approximate location of the degradation within the kinematic chain. More details are available in Refs. [16,28].

The insertion of the key into the PVS is being verified to determine what uncertainty, if any, exists regarding the known tolerances of the fit. For example, if the clearance between the key and the PVS is designed to 25 μm, then the ideal scenario is that the key has a range of motion of 25 μm regarding its insertion into the PVS. Realistically speaking, uncertainties exist including manufacturing tolerances of the key and the PVS, the setup error of the key with respect to the PVS, etc.

As noted earlier, the PVS provides binary output, meaning that the element being tested either passes or fails its specific positioning test. If all elements can insert the key into the PVS, then the workcell is considered healthy to the designed tolerance between the key and the PVS. If an element fails, then that data can be used to determine specifically where within the workcell a change or degradation

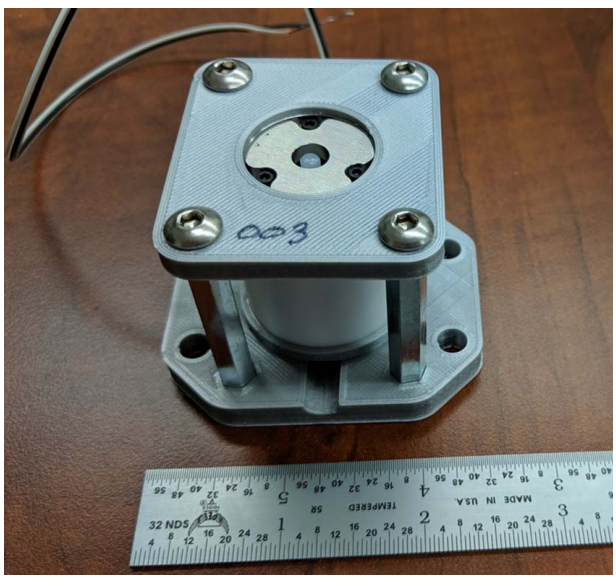

Fig. 2 Position verification sensor with discrete output

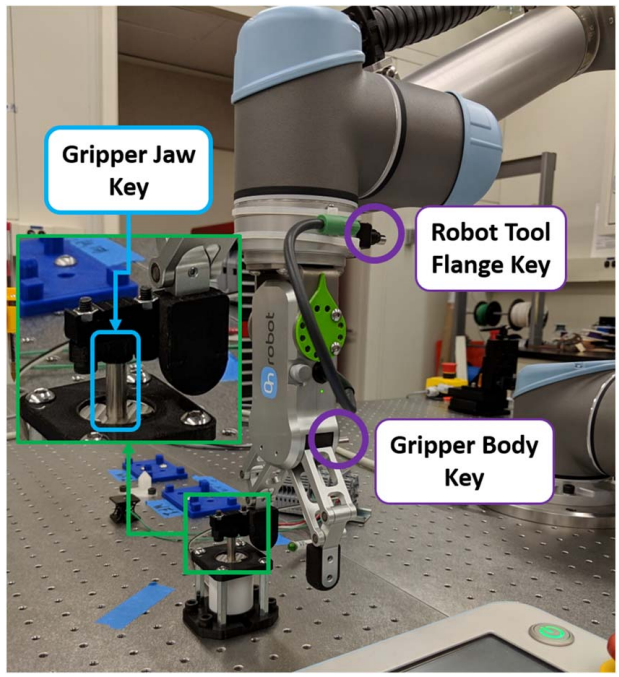

Fig. 3 NIST Testbed key mounting locations

has occurred. By itself, or coupled with other data from the workcell's operations, these data can be used to then efficiently respond to that change. The declaration that the workcell is healthy to the designed tolerance is only true if all uncertainties are known and quantified. If not, for example, a kinematic chain that successfully passes all tests with a tolerance of 25 μm may only be healthy to 50 μm or larger. Whatever it may be, it is critical for the manufacturer to know exactly what they are testing. The verification testing of the PVS is a core step in ultimately determining the uncertainty of the overall test method.

4 Experimental Design

The PVS' performance needs to be verified to understand its capability and measurement uncertainties as it is used within the test method. The PVS is actively being tested to gather this information. A verification test process has been developed using an automated, linear, three-axis stage. The test stand is set up such that a standard key is mounted to the three-axis stage and a PVS is mounted directly below (as shown in Fig. 4). The stage can then be commanded to move and insert the key into the PVS at different locations in an attempt to achieve a positive response from the PVS (i.e., the key is successfully inserted into the sensor). This test stand simulates robot movement with an attempt to insert the key into the PVS and the repeatability uncertainties that exist within them.

This test process was previously performed manually where there was a desire to automate the process because of the manual process being tedious, cumbersome, and susceptible to human error. Stage movement had previously been controlled using manual micrometers, for the *X*- and *Y*-axis, and a lever for the Z-axis (shown in Fig. 5). The *X* and *Y* movements test different locations or points of the sensor while the *Z*-axis movement is used to engage or disengage the key from the PVS. The chosen devices enabled the user to move the stage in increments of 1 μm at a time providing very granular control of the stage's movements. To automate the movement of the stage, the micrometers and lever have been replaced with three motor controllers that are connected to three actuators (shown in Fig. 4). This new hardware has the same range of motion and resolution as the manually driven stage.

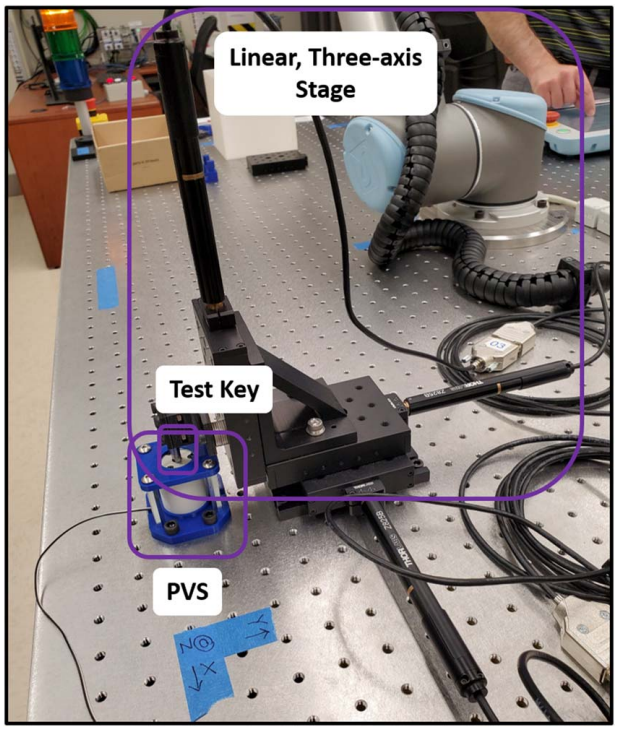

Fig. 4 Automated test stand

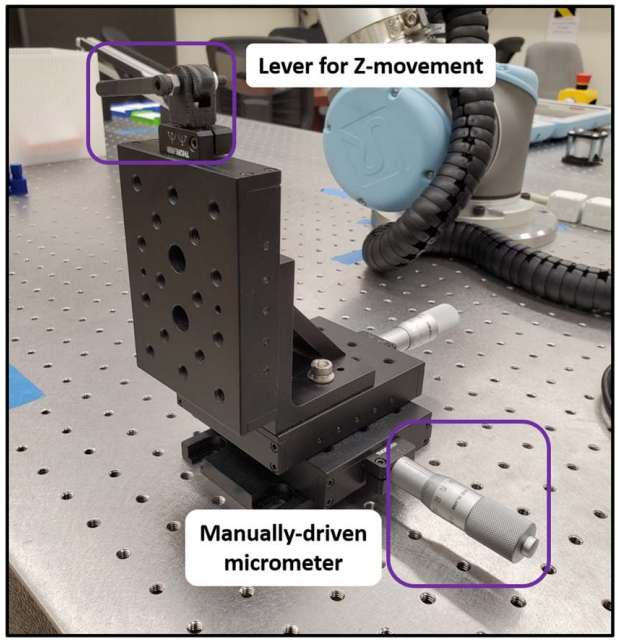

Fig. 5 Manual test stand

A MATLAB program (running off a laptop personal computer (PC) that is connected via a universal serial bus (USB) to the motor controllers of the linear stage) provides a test grid encompassing the top hole of the PVS. This grid consists of points to be tested, with the size and resolution of the grids (i.e., the number of points to be tested and spacing between points) determined by user input. The program then selects the order for which the test points are evaluated by using one of three user-selected methods (i.e., random pattern, vertical movement testing each *Y*-column before moving onto the next, or horizontal movement testing each *X*-row before moving onto the next) and commands the stage to move the key to those points. At each point, the stage will attempt to insert the key into the PVS. The PVS' digital output is connected to an oscilloscope, which is used to determine the success of each attempted insertion. The oscilloscope measures the output voltage of the sensor at each test point, which is then input into the MATLAB program. The oscilloscope is connected to the same PC laptop via USB connection. Upon receiving the signal input from the oscilloscope, the program can determine if the insertion was successful or not based on the captured voltage value (high voltage indicates success). Each test result is recorded within the program. Sample output from the MATLAB is shown in Fig. 6. Movements of the stage are programmed via MATLAB in English Units given the English dimensions of the COTS key.

The results of the insertion at each point are stored, formatted into grids, and exported into MS Excel ®. Each point in the grid contains either a green "1" (indicating a successful test point) or a red "0" (indicated as a failed test point). These grids advance the understanding of how the sensor performs. Due to the circular shape of the mating hole on the sensor, it is expected that the results from each test will be a grid with a tight center circle of successful test points surrounded by unsuccessful test points. Figure 7 present results of random, horizontal, and vertical ordered tests with a 12×12 grid (for 144 total test points) and a stated key and sensor clearance of 25 μm.

5 Testing and Results

Preliminary sensor testing has been performed using this new automated test method. Testing was performed on two unique PVS's that differed in the material of a single internal component;

```
Currently testing point 238 of 397 at x=0.00850 inches and y=0.00550 inches.
The X motor position is 0.0085023622 inches.
The Y motor position is 0.0055015748 inches.
Process Unsuccessful

Currently testing point 328 of 396 at x=0.00500 inches and y=0.00800 inches.
The X motor position is 0.0050007874 inches.
The Y motor position is 0.0080023622 inches.
Process Unsuccessful

Currently testing point 215 of 395 at x=0.00700 inches and y=0.00500 inches.
The X motor position is 0.0070023622 inches.
The Y motor position is 0.0050011811 inches.
Process Successful

Currently testing point 140 of 394 at x=0.00950 inches and y=0.00300 inches.
The X motor position is 0.0095023622 inches.
The Y motor position is 0.0030000000 inches.
Process Unsuccessful
```

Fig. 6 Sample MATLAB output

one sensor's component is made from 3D-printed plastic, and the other sensor's component is made from machined stainless steel (SS). The PVS with the SS component was found to be of much higher precision than the PVS with the 3D-printed plastic component.

Testing of the measurement test stand, along with capturing preliminary verification results of the PVS, began by conducting 55 total tests on a single PVS. These tests consisted of grid size *XX* and resolution *YY*, where *XX* and *YY* are test-specified variables for grid size and resolution, respectively. The order that the individual observations were collected varied across the 55 tests such that 19 tests were collected in random order, 18 tests in vertical order, and 18 tests in horizontal order. Ideally, it is expected that the successful sensor results would create a precise circular pattern, within the resolution of the test grid, with a diameter equal to the diameter of the key. All other areas of the test grid should result in unsuccessful sensor results. The results of the testing done with this PVS deviated from the expected results. The circle of successful test observations encompassed most of the grid as opposed to the tight, expected center region. This led to the dissection of the first PVS revealing the internal 3D-printed component. Given that the parts from this material type are less precise than the parts machined in SS, the SS PVS was then integrated into the measurement test stand. Fifteen total tests were run with the SS PVS: five random order, six vertical order, and four horizontal order; each with grid size $XX = 12$ and resolution $YY = 20.8\ \mu$m. The grids created using this sensor were more closely aligned with what was originally anticipated; the grid was comprised of unsuccessful insertion tests, while the center of the grid was comprised of a tight, circular shape of successful tests. In total, 71 tests have been completed as of the preliminary development of this publication; 25 random order, 24 vertical order, and 22 horizontal order. These tests ranged in size from 12 observations (a very preliminary 3×4 grid to confirm the MATLAB code) to 2500 observations. Test times ranged in duration from about five minutes to about 13 h.

Some tests had unexpected anomalies; there were unsuccessful insertions in the middle of the grid where successful insertions were expected or successful insertions on the outside of the grid where failed insertions were expected. This was a very common problem that was faced throughout the entire testing process. Figure 7 presents three, 12×12 grid test results from random, horizontal, and vertical tests using the SS PVS that had a designed key/sensor tolerance of 25 μm. This means that the PVS opening is nominally 25 μm larger than the diameter of the key. For the specific tests that have been run and are discussed below, the PVS circular opening has a machined tolerance of 6.375 mm−0.0 to +12 μm while the tolerance of the cylinder key is 6.350 mm −0 to +5 μm. The non-binary numbers in Fig. 7 represent the position, in millimeters, in the *X* and *Y* directions of travel from the *X*, *Y* coordinate origin of the key that is mated to the test stand.

Other tests included larger grid dimensions, such as 20×20 grids. Figure 8 presents a composite result of five separate, 20×20 tests that were performed. The results of the five tests were overlaid onto one another. The number provided at each individual point on the grid in Fig. 8 is the number of total tests (out of five) for which a successful insertion was observed. For example, a three represents a 60% success rate where three insertions were successful while two insertions failed at the same point across five separate tests.

6 Discussion

The material that is used to fabricate the two precision components of a single PVS was found to have a significant impact on the result of the test. The PVS with the internal 3D-printed plastic component yields less precise parts as compared to its machined SS counterpart. SS is a much stronger material that can be machined to tight tolerances making it a more advantageous material to use for the PVS's precision components. The PVS with the 3D-printed plastic component has been removed from all further testing and workcell implementations. All PVS' in operation contain precision components made out of machined SS.

Further analysis uncovered additional deficiencies: (1) inconsistencies with the oscilloscope being used, (2) a defective automated linear stage, and (3) the geometry of the key. First, the oscilloscope

Random (in)

0.00902	0	0	0	0	0	0	0	0	0	0	0	0
0.0082	0	0	0	0	0	0	0	0	0	0	0	0
0.00738	0	0	0	0	0	0	1	0	0	0	0	0
0.00656	0	0	0	0	1	1	1	1	1	0	0	0
0.00574	0	0	0	0	1	1	1	1	1	0	0	0
0.00492	0	0	0	1	1	1	1	1	1	0	0	0
0.0041	0	0	0	1	1	1	1	1	1	0	0	0
0.00328	0	0	0	0	1	1	1	1	1	0	0	0
0.00246	0	0	0	0	1	1	1	1	1	0	0	0
0.00164	0	0	0	0	0	1	1	1	0	0	0	0
0.00082	0	0	0	0	0	0	0	0	0	0	0	0
3.03577E-18	0	0	0	0	0	0	0	0	0	0	0	0
	0	0.00082	0.00164	0.00246	0.00328	0.0041	0.00492	0.00574	0.00656	0.00738	0.0082	0.00902

Horizontal (in)

0.00902	0	0	0	0	0	0	0	0	0	0	0	0
0.0082	0	0	0	0	0	0	0	0	0	0	0	0
0.00738	0	0	0	0	0	1	1	1	1	0	0	0
0.00656	0	0	0	0	1	1	1	1	1	0	0	0
0.00574	0	0	0	0	1	1	1	1	1	1	0	0
0.00492	0	0	0	0	1	1	1	1	1	1	0	0
0.0041	0	0	0	0	1	1	1	1	1	1	0	0
0.00328	0	0	0	0	0	1	1	1	1	0	0	0
0.00246	0	0	0	0	0	1	1	1	1	0	0	0
0.00164	0	0	0	0	0	0	1	1	1	0	0	0
0.00082	0	0	0	0	0	0	0	0	0	0	0	0
3.03577E-18	0	0	0	0	0	0	0	0	0	0	0	0
	0	0.00082	0.00164	0.00246	0.00328	0.0041	0.00492	0.00574	0.00656	0.00738	0.0082	0.00902

Vertical (in)

0.00902	0	0	0	0	0	0	0	0	0	0	0	0
0.0082	0	0	0	0	0	0	0	0	0	0	0	0
0.00738	0	0	0	0	1	1	1	1	0	0	0	0
0.00656	0	0	0	1	1	1	1	1	0	0	0	0
0.00574	0	0	0	1	1	1	1	1	1	0	0	0
0.00492	0	0	0	1	1	1	1	1	1	0	0	0
0.0041	0	0	0	0	1	1	1	1	1	0	0	0
0.00328	0	0	0	0	1	1	1	1	1	0	0	0
0.00246	0	0	0	0	0	1	1	1	0	0	0	0
0.00164	0	0	0	0	0	1	1	1	0	0	0	0
0.00082	0	0	0	0	0	0	0	0	0	0	0	0
3.03577E-18	0	0	0	0	0	0	0	0	0	0	0	0
	0	0.00082	0.00164	0.00246	0.00328	0.0041	0.00492	0.00574	0.00656	0.00738	0.0082	0.00902

Fig. 7 Test results from 12 × 12 grid test of a 0.001″ tolerance between the key and SS PVS

that is used to measure the voltage from the PVS sensor would often emit a significant amount of electronic noise. This noise would cause the voltage values from the sensor to fluctuate to a degree that prevented the MATLAB program from discerning between a successful and an unsuccessful insertion test, leading to inaccurate results. Second, additional error stemmed from a breakdown of the linear, multi-axis stage that was used to move the pin to different points. The malfunction of the stage limited its range of motion and prevented it from moving to the desired location when commanded to do so by the MATLAB program, which significantly impacted the results of some of the tests. The malfunctioning stage was replaced with a new, identical stage and testing continued. Lastly, it is important to note that the keys inserted into the PVS are COTS high precision cylinders with notionally known dimensions. Unfortunately,

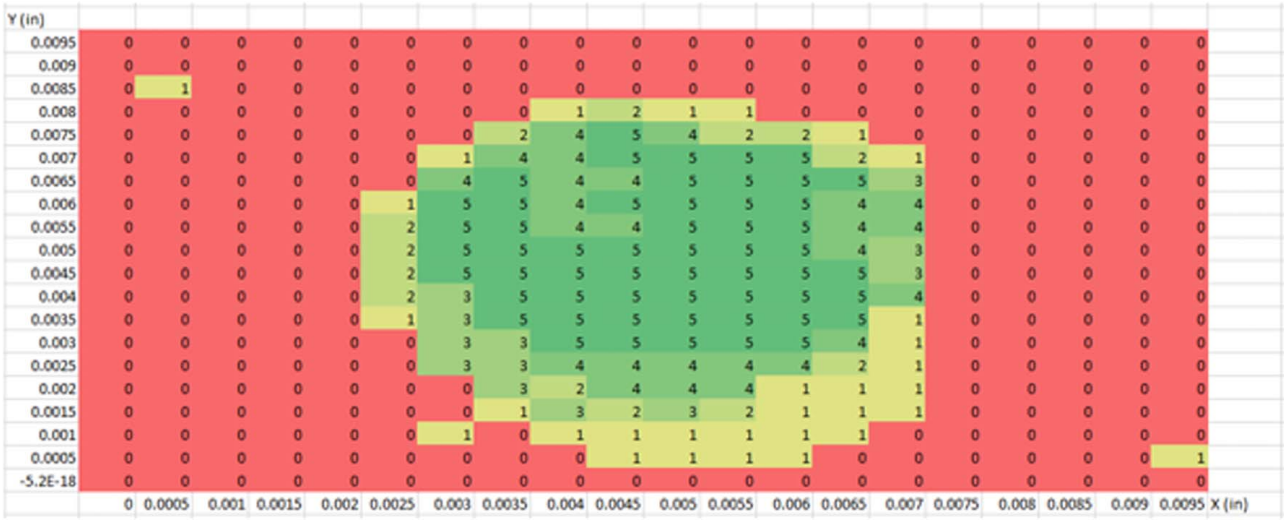

Fig. 8 Composite test results from 20 × 20 grid test of a 0.001″ tolerance between the key and PVS

the cylinder contains a very small chamfer at the cylindrical edges. This chamfer feature likely resulted in several additional boundary test points being successful, as opposed to failing, since this chamfer would allow the pin to "slide in" if the pin was slightly out of tolerance.

The impacts of these deficiencies were obvious for several tests whose results have been discarded entirely; however, the deficiencies may have also affected tests that have been considered "good." The results of the insertion process at one or more points in these "good" tests could have been changed due to these shortcomings. The malfunctioning stage issue has been resolved and will have a minimal effect on future testing. The oscilloscope issue is still being investigated to find a solution to the problem, which may involve changing oscilloscope settings or changing the method used to measure sensor voltage. Regarding the COTS keys with slight chamfer, these keys are still in use until a viable replacement is determined. One potential solution is to machine custom keys of similarly tight tolerances with no chamfer, yet there will have to be some type of finishing operation performed on the edges of the cylinders to remove any sharp edges. This would provide a natural, yet slight chamfer. It is possible that the long-term solution is to continue to use the COTS keys and appropriately adjust the subsequent results. For example, a known, designed tolerance of 25 μm between the COTS key and the PVS could translate into successful insertion test results demonstrating a 63.5-μm tolerance.

The optimal test (i.e., size of grid, spacing between points, and optimal point selection process) for the verification of the PVS is still being determined. Ideally, this verification test would provide enough information on the behavior and integrity of the PVS to generate a quantifiable confidence in its measurement capability and be performed within a reasonable amount of time.

The grid sizes that have been used so far have ranged from 3×4 to 50×50, and the resolution of the spacing between points has ranged from 100 μm to 5 μm. The results of the tests performed at each of these sizes and resolutions varied between the three different selection methods. The three order of data collection methods (random, vertical, and horizontal) were applied at each of grid sizes and resolutions considered. More detailed grids generate additional data on the PVS and its behavior, until a capacity is achieved where no new information can be gathered.

Overall, the preliminary test efforts proved insightful, in terms of developing both an initial understanding of the PVS' performance and the capability of this specific verification test method. From preliminary test results, including several composites that have been produced, it is evident that a key and PVS pairing with a designed 25 μm clearance will have successful insertion tests greater than 25 μm due to the factors discussed earlier in this section.

7 Future Efforts

Before more testing of the PVS can be performed, refinements need to be made to the overall test process including adjusting the oscilloscope to ensure its reliability and characterizing the boundary chamfer of the COTS high precision cylinder (as discussed earlier). After the necessary improvements have been made to the process, testing of the PVS will be required before reaching the end goal of releasing the sensor to industry for ubiquitous use. All the testing that has been performed so far has been done using PVS with the specific clearance of 25 μm relative to the key. Future efforts will involve more testing of sensors with a key clearance of 25 μm, as well as other sensors with larger key clearances (e.g., 50 μm, 100 μm, and 254 μm). With additional testing and improvements, the PVS can be verified for implementation and use in manufacturing environments. The ultimate goal is for the *Identification and Isolation of Robot Workcell Accuracy Degradation* test method and the PVS to be used by industry to monitor and respond to changes in the health of their robot workcells.

The MATLAB program used in the testing process will also be updated to add three new functionalities: a graphical user interface (GUI), an option to test grid boundary conditions (the regions where the test results change from successful to unsuccessful), and an expanded analysis and visualization capability within the MATLAB platform. The GUI will make the testing process more user-friendly for personnel who are not familiar with the program. The GUI is currently in the very early stages of development. The boundary testing functionality will allow the user to move the stage to the boundary points of the center circle and increment outward by very small amounts (less than the distance between points) until reaching a point where the key and sensor are no longer able to mate. This will give the user a more accurate distribution, along with a more accurate representation of how the PVS behaves and crystallizes the PVS' boundaries in terms of where successful tests become unsuccessful. This testing approach will gather new information about the PVS, such as a more accurate representation of the room for error that is acceptable to successfully insert the key into the PVS.

The current PVS that is being used in the test method is a binary sensor. It can communicate to users that an element along the workcell's kinematic chain either passes or fails the test, indicating whether the workcell is healthy or not. A new PVS is being developed with the ability to communicate a greater granularity of

workcell health. For example, the workcell is healthy and no maintenance is needed, the workcell health is degrading but it is not affecting part quality, or the workcell is unhealthy and part quality is negatively impacted (this scenario would require immediate attention). This intelligence would better enable manufacturers to optimize their maintenance efforts and schedules. This new generation of PVS will also require testing and verification. Future efforts will involve using the same, or a similar, process to test and verify this new sensor for release to manufacturers.

Lastly, it is intended that the data from the execution of the *Identification and Isolation of Robot Workcell Accuracy Degradation* test method will augment process and equipment intelligence with respect to health and maintenance activities. The PVS' binary output (pass or fail) of key elements along a robot workcell's kinematic chain could be coupled with one or more of the data types presented in the Background section to enhance overall maintenance intelligence of a manufacturing operation or speed deeper troubleshooting of a workcell. Once the PVS is further verified through additional testing, its continued use within manufacturing facilities will present opportunities to capture binary test method data with real manufacturing data. These data will be correlated to better understand degradation trends and relationships among data types. Identifying redundant or inconsequential data can have a substantial impact on future data collection and analysis efforts. Ideally, manufacturers will only capture data from specific sources to acquire targeted intelligence leading to decisive and cost-effective maintenance actions.

NIST Disclaimer

The views and opinions expressed herein do not necessarily state or reflect those of NIST. Certain commercial entities, equipment, or materials may be identified in this document to illustrate a point or concept. Such identification is not intended to imply recommendation or endorsement by NIST, nor is it intended to imply that the entities, materials, or equipment are necessarily the best available for the purpose.

Nomenclature

V&V = verification and validation

References

[1] Michalos, G., Makris, S., Papakostas, N., Mourtzis, D., and Chryssolouris, G., 2010, "Automotive Assembly Technologies Review: Challenges and Outlook for a Flexible and Adaptive Approach," CIRP J. Manuf. Sci. Technol., **2**(2), pp. 81–91.

[2] Muller, R., Esser, M., and Vette, M., 2013, "Reconfigurable Handling Systems as an Enabler for Large Components in Mass Customized Production," J. Intell. Manuf., **24**(5), pp. 977–990.

[3] Jovane, F., Koren, Y., and Boer, C. R., 2003, "Present and Future of Flexible Automation: Towards New Paradigms," CIRP Ann.-Manuf. Technol., **52**(2), pp. 543–560.

[4] Marvel, J. A., and Newman, W. S., 2009, "Accelerating Robotic Assembly Parameter Optimization Through the Generation of Internal Models," IEEE International Conference on Proceedings of Technologies for Practical Robot Applications, TePRA 2009, Woburn, MA, Nov. 9–10, IEEE, pp. 42–47.

[5] Qiao, G., and Weiss, B. A., 2016, "Advancing Measurement Science to Assess Monitoring, Diagnostics, and Prognostics for Manufacturing Robotics," Int. J. Progn. Health Manage., **7**(Spec Iss on Smart Manufacturing PHM), p. 13.

[6] Park, C., and Park, K., 2008, "Design and Kinematics Analysis of Dual arm Robot Manipulator for Precision Assembly," 6th IEEE International Conference on Proceedings of Industrial Informatics, INDIN 2008, Daejon, South Korea, July 13–16, IEEE, pp. 430–435.

[7] Baglee, D., and Jantunen, E., 2014, "Can Equipment Failure Modes Support the use of a Condition Based Maintenance Strategy?," Proceedings of 3rd International Conference on Through-Life Engineering Services, TESConf, Cranfield, UK, Nov. 4–5, Elsevier, pp. 87–91.

[8] Ly, C., Tom, K., Byington, C. S., Patrick, R., and Vachtsevanos, G. J., 2009, "Fault Diagnosis and Failure Prognosis for Engineering Systems: A Global Perspective," Proceeding of 2009 IEEE International Conference on Automation Science and Engineering, CASE, Bangalore, India, Aug. 22–25, IEEE Computer Society, pp. 108–115.

[9] Williams, R., Banner, J., Knowles, I., Dube, M., Natishan, M., and Pecht, M., 1998, "An Investigation of 'Cannot Duplicate' Failures," Qual. Reliab. Eng. Int., **14**(5), pp. 331–337.

[10] Jin, X., Siegel, D., Weiss, B. A., Gamel, E., Wang, W., Lee, J., and Ni, J., 2016, "The Present Status and Future Growth of Maintenance in US Manufacturing: Results From a Pilot Survey," Manuf. Rev. (Les Ulis), **3**(10), p. 10.

[11] Helu, M., and Weiss, B. A., 2016, "The Current State of Sensing, Health Management, and Control for Small-to-Medium-Szed Manufacturers," Proceedings of ASME Manufacturing Science and Engineering Conference, MSEC2016, Blacksburg, VA, June 27–July 1.

[12] Weiss, B. A., Vogl, G. W., Helu, M., Qiao, G., Pellegrino, J., Justiniano, M., and Raghunathan, A., 2015, "Measurement Science for Prognostics and Health Management for Smart Manufacturing Systems: Key Findings From a Roadmapping Workshop," Annual Conference of the Prognostics and Health Management Society 2015, P. Society, ed., PHM Society, Coronado, CA, Nov. 19–20, 2014, p. 11.

[13] Pellegrino, J., Justiniano, M., Raghunathan, A., and Weiss, B. A., 2016, *Measurement Science Roadmap for Prognostics and Health Management for Smart Manufacturing Systems*, NIST Advanced Manufacturing Seriess (AMS), Gaithersburg, MD.

[14] Helu, M., and Hedberg, T., 2015, "Enabling Smart Manufacturing Research and Development Using a Product Lifecycle Test Bed," Proceedings of 43rd North American Manufacturing Research Conference, Namrc 43, Charlotte, NC, June 8–12, Vol. 1, pp. 86–97.

[15] Klinger, A. S., and Weiss, B. A., 2018, "Robotic Work Cell Test Bed to Support Measurement Science for PHM," 2018, ASME Manufacturing Science and Engineering Conference (MSEC), College Station, TX, June 18–22, American Society of Mechanical Engineers (ASME).

[16] Klinger, A., and Weiss, B. A., 2018, "Examining Workcell Kinematic Chains to Identify Sources of Positioning Degradation," Annual Conference of the PHM Society, Philadelphia, PA, p. 9.

[17] Jin, X., Weiss, B. A., Siegel, D., and Lee, J., 2016, "Present Status and Future Growth of Advanced Maintenance Technology and Strategy in US Manufacturing," Int. J. Progn. Health Manage., **7**(Spec Iss on Smart Manufacturing PHM), p. 012.

[18] Brundage, M. P., Sexton, T., Hodkiewicz, M., Morris, K. C., Arinez, J., Ameri, F., Ni, J., and Xiao, G., 2019, "Where do we Start? Guidance for Technology Implementation in Maintenance Management for Manufacturing," ASME J. Manuf. Sci. Eng., **141**(9), p. 091005.

[19] Baybutt, M., Minnella, C., Ginart, A., Kalgren, P. W., and Roemer, M. J., 2007, "Improving Digital System Diagnostics Through Prognostic and Health Management (PHM) Technology," Proceedings of 42nd Annual IEEE AUTOTESTCON Conference, Baltimore, MD, Sept. 17–20, Institute of Electrical and Electronics Engineers Inc., pp. 537–546.

[20] Holland, S. W., Barajas, L. G., Salman, M., and Zhang, Y., "PHM for Automotive Manufacturing & Vehicle Applications," Proceedings of Prognostics & Health Management Conference, Portland, OR, Oct. 10–16.

[21] Tsui, K. L., Chen, N., Zhou, Q., Hai, Y. Z., and Wang, W. B., 2015, "Prognostics and Health Management: A Review on Data Driven Approaches," Math. Prob. Eng., **2015**, pp. 1–17.

[22] Vogl, G. W., Weiss, B. A., and Donmez, M. A., 2014, "Standards Related to Prognostics and Health Management (PHM) for Manufacturing," No. NISTIR 8012, National Institute of Standards and Technology (NIST), Gaithersburg, MD.

[23] Vogl, G. W., Weiss, B. A., and Helu, M., 2019, "A Review of Diagnostic and Prognostic Capabilities and Best Practices for Manufacturing," J. Intell. Manuf., **30**(1), pp. 79–95.

[24] Sharp, M., Brundage, M. P., Sprock, T., and Weiss, B. A., "Selecting Optimal Data for Creating Informed Maintenance Decisions in a Manufacturing Environment," Proceedings of Model-Based Enterprise Summit 2019, Gaithersburg, MD, Apr. 1–4, pp. 121–130.

[25] Pan, M. C., Van Brussel, H., and Sas, P., 1998, "Intelligent Joint Fault Diagnosis of Industrial Robots," Mech. Syst. Signal Process., **12**(4), pp. 571–588.

[26] Qiao, G., Schlenoff, C. I., and Weiss, B. A., 2017, "Quick Positional Health Assessment for Industrial Robot Prognostics and Health Management (PHM)," IEEE International Conference on Robotics and Automation 2017, Singapore, May 29–June 3, p. 6.

[27] Weiss, B. A., and Klinger, A. S., 2017 "Identification of Industrial Robot Arm Work Cell Use Cases and a Test Bed to Promote Monitoring, Diagnostic, and Prognostic Technologies," Proceedings of Annual Conference of the Prognostics and Health Management (PHM) Society, St. Petersburg, FL, Oct. 2–5, PHM Society, p. 9.

[28] Weiss, B. A., 2019, "Developing Measurement Science to Verify and Validate the Identification of Robot Workcell Degradation," ASME 2019 14th International Manufacturing Science and Engineering Conference (MSEC2019), June 10–14, ASME, Erie, PA, p. 10.